Theor Chem Acc (2006) 116: 718–725
DOI 10.1007/s00214-006-0118-0

REGULAR ARTICLE

Paul Fleurat-Lessard · François Volatron

Theoretical study of the distortion from regular tetrahedral structure of $M(NH_2)_4$ complexes

Received: 19 December 2004 / Accepted: 26 January 2005 / Published online: 23 March 2006
© Springer-Verlag 2006

Abstract Theoretical study on tetrakis-amido complexes ($M(NR_2)_4$, M = Ti, V, Cr, and Mo; R = H, Me) is presented. At first a rough investigation of the potential energy surface indicates that all stationary points are of S_4 or D_2 symmetry depending on the coupled rotations of the NR_2 groups. Qualitative correlation diagrams are calculated within S_4 or D_2 symmetry constraint between two limiting structures of D_2d symmetry. DFT (B3LYP) calculations on these two paths are presented for unsubstituted complexes (R = H) and the various minima are optimized and characterized. These results are discussed in the light of the correlation diagrams. Finally, optimization of the different minima has been performed on substituted species (R = Me) and the theoretical results are shown to be in good agreement with the experimental structural determination when available.

1 Introduction

Replacement of hydrogen atoms or alkyl substituents by π-donor substituents may have a dramatic effect on the structure and the reactivity of molecules. A prototypical example of mono-faced π-donor substituent is the amido radical NR_2 which is widely used in organic, inorganic, and organometallic chemistry. For instance, tetrakis-dimethyl-amino ethylene $(Me_2N)_2C = C(NMe_2)_2$ exhibits a rather surprising structure in which the four amino planes rotate by about 55° with respect to the ethylenic plane [1,2]. In addition, the rotations of the four amino groups occur in a conrotatory manner. We have shown by theoretical calculations that this surprising geometry results from a balance between electronic and steric effects [3]. Similar conclusions have been reached in the study of tri-coordinated aluminum species [4] and metallic $M(NR_2)_3$ species [5].

In this paper we address the geometrical and electronic structure of tetrakis-amido transition metal complexes. Our aim is to understand the geometrical structure of such complexes and to give a rationale of their electronic structure. To our knowledge, tetrakis $M(NR_2)_4$ complexes have been synthesized for M = Ti, V, Cr, Zr, Nb, Mo, and Hf. Since the pioneer work of Bradley and coworkers [6], structural studies have been carried out by electron diffraction (ED) for $Zr(NMe_2)_4$ [7], $Ti(NMe_2)_4$ and $V(NMe_2)_4$ [8] and by X-ray study for $Mo(NMe_2)_4$ [9], and $V(NMe_2)_4$ [10]. Among all these structural determinations common features are found in these complexes: (1) the MN_4 core is nearly tetrahedral, (2) the NC_2 moiety is roughly planar.

When one considers the $M(NC_2)_4$ framework, the symmetry is reduced with respect to the tetrahedral symmetry of the MN_4 core. Two limiting structures have been already pointed out in experimental studies. In the first one, ($D_{2d}0$, **1**), the four NC_2 planes belong to two orthogonal MN_2 planes. In the second structure, ($D_{2d}90$, **2**), they are orthogonal to these MN_2 planes. Both structures belong to the D_{2d} symmetry point group.

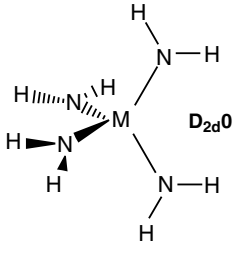

1

P. Fleurat-Lessard · F. Volatron (✉)
Laboratoire de Chimie Physique (CNRS-UMR8000),
Université de Paris-Sud, Bât. 490, 91405 Orsay Cedex, France
E-mail: paul.fleurat-lessard@ens-lyon.fr
E-mail: volatron@lct.jussieu.fr

Present address: P. Fleurat-Lessard
Laboratoire de Chimie, Ecole Normale Supérieure de Lyon,
46, Allée d'Italie, 69364 Lyon Cedex 07, France

Present address: F. Volatron
Laboratoire de Chimie Théorique,
Faculté des Sciences de Jussieu Université Paris VI,
3 rue Galilée, 94200 IVRY, France

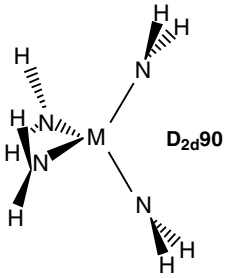

2

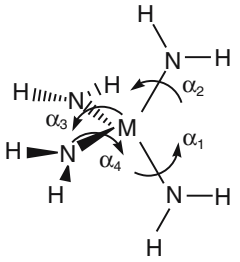

3

Coupled rotations of the NC_2 planes around the M–N bonds are experimentally observed and lead to lower symmetry structures. This rotational angle is found to be equal to 51° and 71° in $Ti(NMe_2)_4$ and $V(NMe_2)_4$, respectively (ED study). Two values (109.7° and 127.7°) were proposed in the $Zr(NMe_2)_4$ case with a large uncertainty. Finally, X-ray diffraction study of $V(NMe_2)_4$ and $Mo(NMe_2)_4$ leads to an almost perfect $D_{2d}90$ structure.

In addition to the structural determination briefly summarized above, another puzzling fact emerges from the experimental data: $Mo(NMe_2)_4$ is found to be diamagnetic whereas $Cr(NEt_2)_4$ is found to be paramagnetic [11]. A simple explanation of this difference should be the well-known larger affinity of Mo for low spin situations with respect to that of Cr. However, one may wonder if geometrical distorsions could play a noticeable role in this different behavior.

To give some light on these different questions, a theoretical DFT study has been undertaken on these complexes.

2 Theoretical methods

The B3LYP DFT method has been used throughout with the help of GAUSSIAN 98 and GAUSSIAN 03 sets of programs [12,13]. For metal atoms, the standard LANL2DZ basis set containing electron core potential and augmented with polarization functions [14] has been used. The ligands atoms have been described with the 6-31G* polarized basis set. All structures have been optimized through an analytical gradient method; the obtained stationary points have been characterized by frequencies calculations.

3 Results

3.1 Exploration of the PES

We have first considered the model molecules $M(NH_2)_4$. The four NH_2 rotational angles (α_1, α_2, α_3, and α_4) are defined in **3**: when all the α_i angles are equal to zero, one gets the $D_{2d}0$ structure. When all these angles are equal to 90°, one gets the $D_{2d}90$ structure.

All geometries with α_i = 0, 30, 60, 90, 120, and 150° (i = 1, 2, 3, and 4) have been generated (about 1,300 structures). Symmetry considerations reduce this large number to 70 different geometries. All of them have been optimized for M = Ti, V, Cr (singlet and triplet), and Mo (singlet and triplet) at the B3LYP/LANL2DZ level under two geometrical constraints: the NH_2 amido groups have been kept planar and the MN_4 core has been frozen in a tetrahedral geometry. In each case, optimization of the α_i leads to only one minimum. Surprisingly the optimized values obtained for α_i in the different minima are strongly coupled. We obtained $\alpha_1=\alpha_2=\alpha_3=\alpha_4$ (M = Cr(S) and Mo(S)) and $\alpha_1=\alpha_2=-\alpha_3=-\alpha_4$ (M = Ti, V, Cr(T) and Mo(T)). In each case, the amido groups defined by α_1 and α_2 are moving conrotatorily as well as those defined by α_3 and α_4. The essential difference between the two kinds of minima found is the overall symmetry of the structure. For ($\alpha_1=\alpha_2=\alpha_3=\alpha_4$) and ($\alpha_1=\alpha_2=-\alpha_3=-\alpha_4$), the structure belongs to the D_2 and S_4 symmetry point group, respectively. Note that these two arrangements have already been considered by Haaland et al. in the study of $Ti(NMe_2)_4$ and $V(NMe_2)_4$ by ED [9]. From the results of this preliminary study and for sake of simplicity, we will only present the $D_{2d}0 \rightarrow D_{2d}90$ interconversion within the D_2 and S_4 symmetry constraint in the following.

3.2 Qualitative study

EHT calculations have been performed in the Titanium case [15] and will be used as a guideline for the two interconversion paths. At first the two D_{2d} geometries will be described. In the $D_{2d}0$ structure, three d orbitals are located high in energy (b_2 and e) while two are lower in energy (a_1 and b_1). On the whole, this d-block structure resembles that of a tetrahedron (three over two); the main difference arises from the interaction of the π lone pairs of the amido groups with the low lying d orbitals. The d_{z2} orbital is not affected whereas the d_{x2-y2} is destabilized by this interaction (**4**). At the EHT level of calculations, the energy difference between these two orbitals is equal to 1.4 eV a gap noticeably smaller than that between d_{z2} and the b_2(or e) orbitals (about 3.1 eV).

4

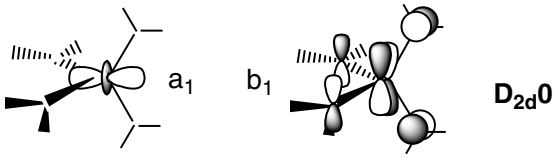

An inverse situation is found in the $D_{2d}90$, structure: the d_{z2}orbital is now destabilized by the amido π lone pairs while the d_{x2-y2} orbital do not interact with them (**5**). The energy gap between these two orbitals is again found to be close to 1.4 eV. In both cases, the three high lying orbitals (which are of t_2 symmetry in the tetrahedron) are nearly degenerate, their energy differences being less than 0.05 eV.

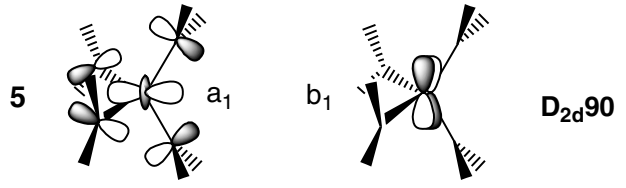

The main difference between the two correlation diagrams between $D_{2d}0$ and $D_{2d}90$ structures comes from the evolution of the two lowest d orbitals (d_{z2} and d_{x2-y2}). In the D_2 symmetry point group, both are of A symmetry and no crossing occurs along the deformation path: a smooth transformation of d_{z2} into d_{x2-y2} (and vice-versa) occurs during the coupled rotation by mixing these two orbitals. In contrast, in the S_4 symmetry point group, the d_{z2} and d_{x2-y2} orbitals are of A and B symmetry, respectively. Crossing between the two correlation lines is allowed and indeed occurs in this correlation diagram (Fig. 1).

3.3 DFT calculation on D_2 and S_4 paths

To give more detailed information on these correlation diagrams, DFT calculations have been undertaken in each case (Ti, V, Cr(S), Cr(T), Mo(S), Mo(T)). For each metal, the two rotational paths in D_2 symmetry ($\alpha_1 = \alpha_2 = \alpha_3 = \alpha_4$) and in S_4 symmetry ($\alpha_1 = \alpha_2 = -\alpha_3 = -\alpha_4$) have been computed by increasing the α_i value by steps of 10°, all the other geometrical parameters being optimized. The minima found on these rotational curves have been fully optimized and characterized. In each case, the energy of the $D_{2d}90$ structure is taken as a reference. The numbering of nitrogen atoms is given in **6**.

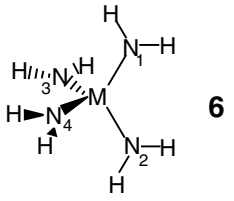

3.3.1 Results

$Ti(NH_2)_4$

The D_2 and S_4 rotational curves are depicted in Fig. 2.

One minimum is found on each curve and has been fully optimized and characterized as well as the limiting structures $D_{2d}0$ and $D_{2d}90$. The results are given in Table 1.

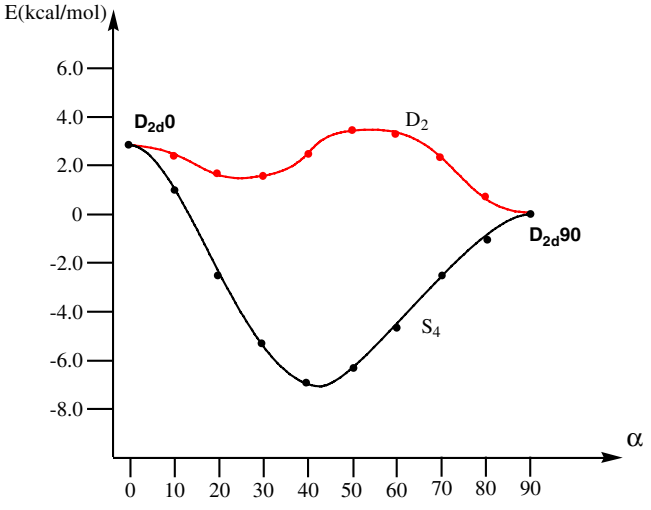

Fig. 2 Optimized deformation paths of D_2 and S_4 symmetry in the Titanium case

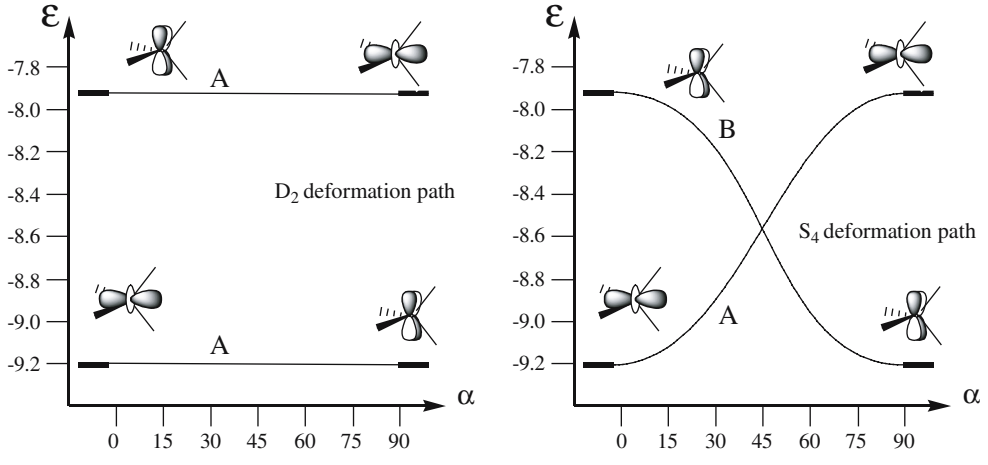

Fig. 1 Correlation diagram of the two lowest d orbitals for the D_2 and S_4 deformation paths. Orbital energies (from EHT calculations) are in eV

Table 1 Main geometrical parameters (bond in Å, angles in degrees) and relative energies (in kcal/mol) of various minima of $Ti(NH_2)_4$

	$D_{2d}0$	$D_{2d}90$	Min D_2	Min S_4
α	0.0	90.0[a]	39.8	39.4
Ti–N	1.903	1.904	1.904	1.898
N_1TiN_2	103.2	119.3	104.8	108.3
N_1TiN_3	112.7	104.8	119.4	110.1
ΔE(kcal/mol)	2.7	0[b]	−2.1	−6.9
Nature	3-SP	–	3-SP	Min

[a] Frozen value
[b] Absolute energy is −282.01807 a.u

Only the S_4 structure has been characterized as a true minimum. Note that this structure of S_4 symmetry is close to that determined theoretically by Schlegel et al. (NTiN = 108.2°; Ti–N = 1.904 Å; $\alpha = 42.5°$) [16].

$V(NH_2)_4$

As in the Titanium case, the two rotational energy curves have been computed and the results are given in Fig. 3.

The D_2 rotational curve is very similar to that obtained in the Titanium case. This is in accordance with the qualitative correlation diagram depicted in Fig. 1: the lowest d-block orbital energetical evolution is flat along the D_2 rotational curve. As a consequence, the energetical contribution of the single d electron in the Vanadium complex is expected to be small and the overall rotational D_2 curve resembles that obtained in the Titanium case.

In contrast, the qualitative correlation diagram in the S_4 motion (Fig. 1) indicates that a symmetry-allowed crossing occurs between the two lowest energy d-block orbitals. Computed rotational curves actually reflect this behavior: two different states have been obtained and the associated rotational curves cross around 35°. On the whole, both curves are repulsive: from $D_{2d}0$ the ^2A state raises in energy and the ^2B state raises in energy from $D_{2d}90$ (Fig. 3) [17].

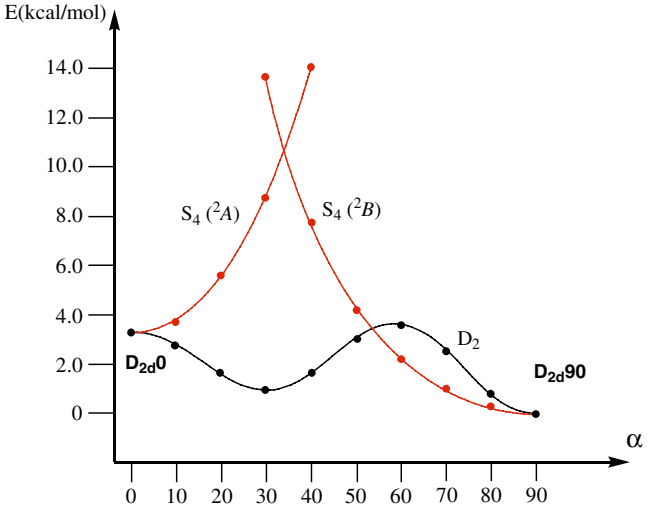

Fig. 3 Optimized deformation paths of D_2 and S_4 symmetry in the Vanadium case

Only two minima appear on these curves. On the D_2 curve a minimum is found ($\alpha = 30.0°$, ΔE=1.1 kcal/mol) and the $D_{2d}90$ structure is found to be the minimum on S_4 curves. Both minima and the $D_{2d}0$ geometry have been fully optimized and characterized. The results are given in Table 2.

$Cr(NH_2)_4$

The D_2 and S_4 rotational energy curves are given in Fig. 4a,b for singlet and triplet states respectively.

The singlet curves are very similar to those obtained in the Vanadium case: along the D_2 path, the ground state of the $D_{2d}0$ structure gently leads to the $D_{2d}90$ geometry in agreement with the qualitative study given in Fig. 1. Two S_4 rotational energy curves are obtained depending on the starting point. Since the two configurations (a^2 and b^2) may interact, MCSCF calculations have been performed. The result of the interaction between these two configurations indicates that the resulting state remains higher in energy than the corresponding D_2 geometry. We therefore only performed geometry optimizations on the limiting structures and the D_2 minimum. The results are given in Table 3.

The triplet curves are slightly more complicated: from the above qualitative study, one would expect a smooth transformation from $D_{2d}0$ to $D_{2d}90$ within D_2 and S_4 deformation since both d_{z2} and d_{x2-y2} orbitals should be occupied by one electron (Fig. 1).

This is not the case for the D_2 deformation curves because of the electronic structure of the $D_{2d}0$ geometry. Surprisingly, the $^3B_1(d^1_{z2}d^1_{xy})$ [18] configuration is found to be the ground state of this geometry instead of the $^3A(d^1_{z2}d^1_{x2-y2})$, which is located 8.3 kcal/mol above the ground state. This energy inversion may originate from a larger π repulsion in the Chromium case than in the Vanadium or Titanium cases. As a consequence, along the D_2 deformation path, the $D_{2d}0$ ground state ($^3B_1$) correlates with a high energy configuration while the $^3A\,D_{2d}90$ ground state ($d^1_{z2}d^1_{x2-y2}$) correlates with the first excited configuration in the $D_{2d}0$ geometry (Fig. 4b, red and blue curves respectively). In addition, another excited configuration ($^3B_3$, $d^1_{z2}d^1_{yz}$) becomes of low energy for rotational angles between 50° and 80° that complicates even further the D_2 energetical deformation curves (fig. 4b, green curve).

In contrast, in the S_4 rotational energy curve, the two orbitals d_{xy} and d_{x2-y2} are both of B symmetry and may

Table 2 Main geometrical parameters (bond in Å, angles in degrees) and relative energies (in kcal/mol) of various minima of $V(NH_2)_4$

	$D_{2d}0$	$D_{2d}90$	Min D_2
α	0	90[a]	30.0
V–N	1.850	1.850	1.852
N_1VN_2	106.4	116.6	105.6
N_1VN_3	111.0	106.0	111.4
ΔE(kcal/mol)	5.2	0	−1.6
Nature	TS	–	Min

[a] Frozen value
[b] Absolute energy is –295.22113 a.u

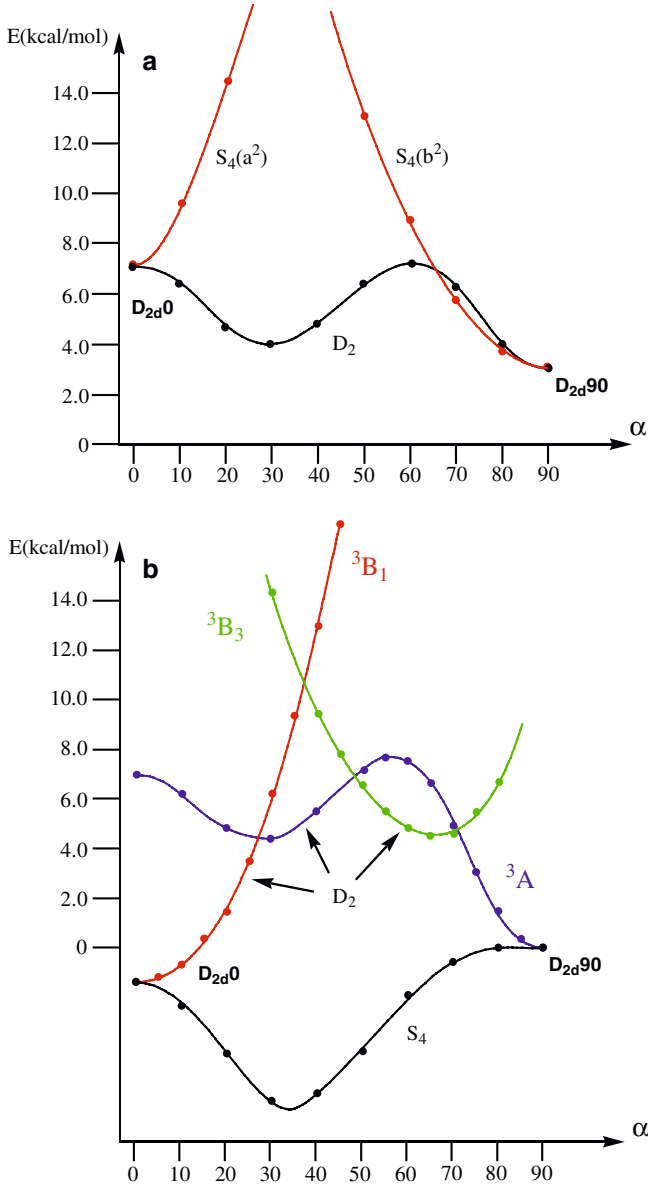

Fig. 4 (**a**) Optimized deformation paths of D_2 and S_4 symmetry in the singlet Chromium case. The origin of the energies is that of the $D_{2d}90$ structure (*triplet state*)
(**b**) Optimized deformation paths of D_2 and S_4 symmetry in the triplet Chromium case. The origin of the energies is that of the $D_{2d}90$ structure

mix along the deformation path. As a consequence, the two ground states ($d^1_{z2}d^1_{xy}$ in $D_{2d}0$ and d^1_{z2} d^1_{x2-y2} in $D_{2d}90$) directly correlate along this reaction path (Fig. 4b black curve).

The $D_{2d}0$ and $D_{2d}90$ limiting structures have been optimized as also the S_4 minimum. The results are given in Table 4.

It should be noted in the Chromium case that both optimized limiting structures are lower in energy in the triplet state than in the singlet state. In addition, the optimized S_4 triplet minimum is 7 kcal/mol lower than the D_2 singlet minimum.

$Mo(NH_2)_4$

The singlet and triplet rotational curves are reported in Figs. 5a, b, respectively. The energetic rotational curves display similar behaviors as those obtained in the Chromium case. In the singlet case, S_4 motion leads to two configurations (a^2 and b^2), which may interact whereas the D_2 motion is an allowed transformation.

In the triplet state (Fig. 5b), D_2 motion again involves three configurations: the $D_{2d}0$ ($^3B_1$) [18] and the $D_{2d}90$ (^3A) ground states as well as the $^3B_3$configuration which becomes of low energy for angles in the range of 40°–80°. Again the S_4 motion smoothly correlates the ground states of the two geometries.

The limiting structures (singlet and triplet) and the two lowest minima (D_2 singlet and S_4 triplet) have been optimized. The results are given in Table 5.

3.3.2 Discussion

From the different results with the various metals, the validity of the correlation diagram depicted in Fig. 1 may be emphasized: the D_2 deformation path predicts a flat energetic evolution of the lowest energy d orbital. Actually, when this orbital is filled with 0 (Ti), 1 (V), or 2 (Cr(T) and Mo(T)) electrons, the energetical evolution is similar for all complexes as shown in Fig. 6. It represents partly the change in the NH_2 pairs repulsions along the deformation path.

From the results in the Titanium case, this evolution is more favorable in S_4 deformation since a deep minimum is found (see Fig. 2). This motion is therefore expected to be the most favorable one as long as the d electrons evolution does not lead to high energies. Such destabilization is expected (Fig. 1) for d^1 and singlet d^2 configurations, i.e., in

Table 3 Main geometrical parameters (bond in Å, angles in degrees) and relative energies (in kcal/mol) of various minima of singlet $Cr(NH_2)_4$

	$D_{2d}0$	$D_{2d}90$	Min D_2
α	0	90[a]	44.1
Cr–N	1.802	1.801	1.804
N_1CrN_2	107.8	115.9	106.8
N_1CrN_3	110.3	106.4	115.2
ΔE(kcal/mol)	7.2	3.1	−5.1
Nature	TS	–	Min

[a] Frozen value

Table 4 Main geometrical parameters (bond in Å, angles in degrees) and relative energies (in kcal/mol) of various minima of triplet $Cr(NH_2)_4$

	$D_{2d}0$	$D_{2d}90$	Min S_4
α	0	90[a]	48.9
Cr–N	1.835	1.832	1.835
N_1CrN_2	93.9	126.8	100.5
N_1CrN_3	117.8	101.6	114.1
ΔE(kcal/mol)	−6.4	0[b]	−12.1
Nature	TS	–	Min

[a] Frozen value
[b] Absolute energy is −310.12500 a.u

Table 5 Main geometrical parameters (bond in Å, angles in degrees) and relative energies (in kcal/mol) of various minima of singlet and triplet states of $Mo(NH_2)_4$.

	Singlet			Triplet		
	$D_{2d}0$	$D_{2d}90$	Min D_2	$D_{2d}0$	$D_{2d}90$	Min S_4
α	0	90[a]	41.4	0	90[(a)]	48.9
Mo–N	1.942	1.941	1.943	1.971	1.832	1.835
N_1MoN_2	109.2	112.2	107.8	89.9	126.8	100.5
N_1MoN_3	109.6	108.1	112.8	120.0	101.6	114.1
ΔE(kcal/mol)	1.3	0[b]	−3.1	12.2	14.6	8.1
Nature	TS	–	Min	TS	–	Min

[a] Frozen value
[b] Absolute energy is −291.38169 a.u

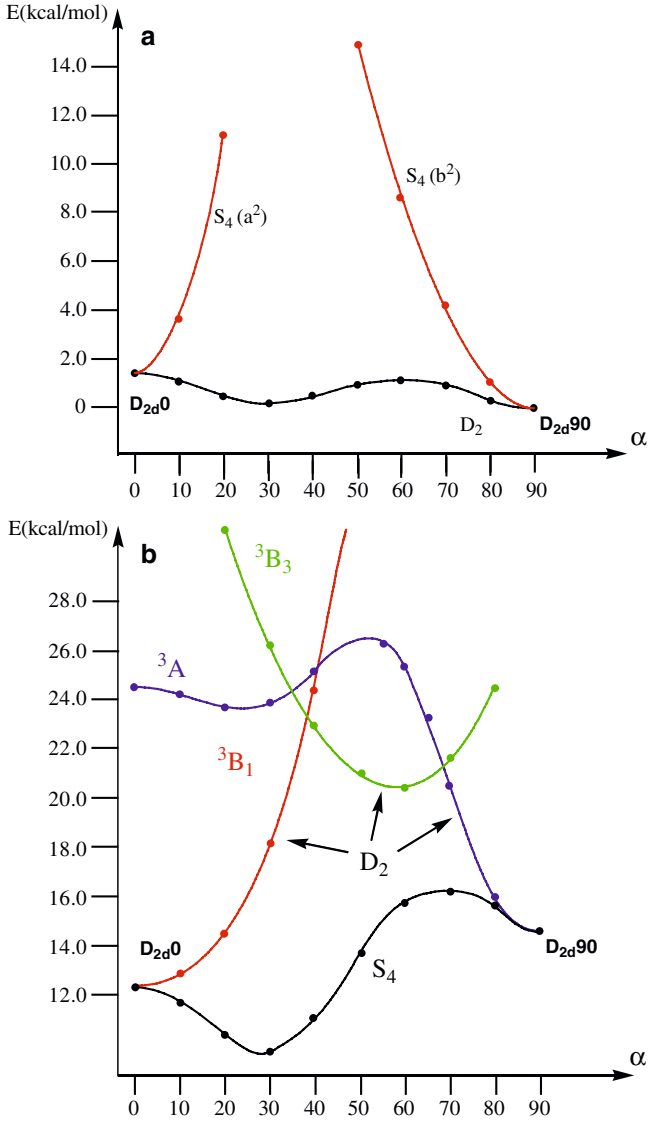

Fig. 5 (**a**) Optimized deformation paths of D_2 and S_4 symmetry in the singlet Molybdenum case
(**b**) Optimized deformation paths of D_2 and S_4 symmetry in the triplet Molybdenum case. The origin of the energies is that of the $D_{2d}90$ structure (*singlet state*)

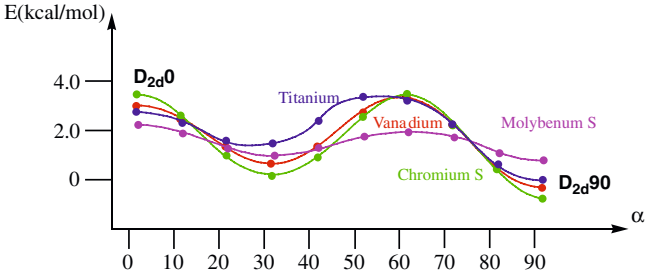

Fig. 6 D_2 deformation paths for the various metal. The origin of the energetical scale is arbitrary

Vanadium and singlet Chromium or Molybdenum cases. In these cases, no S_4 minimum has been found (Figs. 3, 4a and 5a). In other cases, the lowest energy structure results from a S_4 deformation.

Another interesting point concerns the structure of the minimum, which has been found for α values around 30° in all the cases depicted in Fig. 6. In fact, due to the high symmetry of these species, if the NMN angles are tetrahedral this structure is equivalent to $D_{2d}90$, the N_1 and N_3 atoms being exchanged. The lower energies of the Min D_2 structures with respect to those of $D_{2d}90$ are due to the full optimization of these structures, the α angle being frozen to 90° in $D_{2d}90$.

A last comment concerns the spin state in the d^2 cases: the absolute minimum for the Chromium complex is the triplet S_4 minimum. On the other hand, the absolute minimum in the Molybdenum case is the D_2 minimum in singlet state. Our results on unsubstituted systems are therefore in accordance with the experimental data.

Table 6 Relative energies (in kcal/mol) of the various optimized geometries depending on the nature of the metal and of its spin state

	$D_{2d}0$	$D_{2d}90$	Min D_2	Min S_4
Ti	6.0	0	0.0	−9.9
V	11.2	0	–	–
Cr(S)	7.5	0	−0.2	–
Cr(T)	1.8	1.4	1.0	−13.1
Mo(S)	2.8	0	−3.4	–
Mo(T)	37.4	28.7	19.4	10.4

Table 7 Comparison between theoretical and experimental geometrical parameters (bond in Å, angles in degrees)

	Titanium		Vanadium			Molybdenum		Chromium
	Min S_4	Exp[a]	$D_{2d}90$	Exp[a]	Exp[b]	Min D_2 (S)	Exp[c]	Min S_4 (T)
M–N	1.916	1.917	1.873	1.879	1.879	1.959	1.926[d]	1.856
α	44.0	51	90.0	71	90.0	90.0	90.0	31.0
N–C[d]	1.456	1.461	1.456	1.457	1.457	1.460	1.466[d]	1.453
N_1MN_2	109.2	114.2	108.5	100.6	112.2	109.7	109.5[d]	103.2
N_1MN_3	109.6	107.2	111.3	114.1	108.1	109.7	109.5[d]	112.7
MNC1	128.1	124.3	122.5	123.2	122.7	123.3	124.0[d]	124.0
MNC2	120.9	124.3	122.8	123.2	122.7	123.3	124.0[d]	120.5

[a] Ref. 8
[b] Ref. 10
[c] Ref. 9
[d] Averaged values

3.4 Calculations on substituted species

Since the experimentally determined structures involve methylated species that are of moderate sizes, optimizations of these species have been performed. In each case the two limiting structures $D_{2d}0$ and $D_{2d}90$ have been reoptimized. The minima that we found for the unsubstituted systems have also been reoptimized, i.e., D_2 and S_4 in Ti, Cr(T) and Mo(T) cases, and D_2 in V, Cr(S) and Mo(S) cases. The relative energies of these extrema are given in Table 6.

From the results given in Table 6, the following conclusions may be drawn. (1) The absolute minimum is of S_4 symmetry in the Titanium case. (2) The $D_{2d}90$ geometry is the most stable one for Vanadium (3) In the Chromium case, the triplet minimum in S_4 geometry is noticeably lower in energy (by about 13 kcal/mol with respect to the lowest energy singlet structure) and is expected to be actually the real minimum for this species. (4) For Molybdenum, the lowest energy structure in the triplet state (Min S_4) is more than 13 kcal/mol above the Min D_2 in the singlet state. This last structure is therefore the absolute minimum in Molybdenum case.

When available, the experimental data of these complexes have been reported in Table 7 together with our theoretical results.

The agreement between computed and experimental values is rather fair in the Titanium case. The main discrepancy concerns the NMe_2 rotational angle which we found equal to 44.0° (51° from experimental determination). Experimental and theoretical results are again in very good agreement in the Vanadium case. It should be noted that, depending on the structural determination method, the α rotational angle is found to be equal to 71° (ED) and 90° (X-ray). Our results are more in favor of X-ray rather than ED determination. Since no experimental determination is available for chromium complex, our results may be viewed as a reasonable prediction for this complex: it is predicted to be a triplet state of S_4 symmetry (Table 7). Finally, the theoretical and experimental determinations agree well for the $Mo(NMe_2)_4$ structure [19]. Our lowest energy structure corresponds to a singlet state in agreement with the diamagnetic nature of the complex. In addition, the Molybdenum environment is found to be almost tetrahedral both from experimental determination ant theoretical calculations.
Note however that we find a rather long Mo–N bond length (1.959 Å) compared with that experimentally found (1.917–1.934 Å, 1.926 Å averaged).

The last comment concerns the spin states of Cr and Mo complexes. Although no structural determination is available for Cr complex, it has been shown that $Cr(NEt_2)_4$ is paramagnetic (triplet state) whereas $Mo(NMe_2)_4$ is diamagnetic. Our results agree well with these experimental data: in the Chromium case, the lowest energy structure is a triplet state of S_4 symmetry and in the Mo case, it is a singlet state of D_2 symmetry (in fact a $D_{2d}90$ structure) [19]. Note that an analogous difference has already been found in the unsubstituted species. In the Chromium case the triplet curves (for instance the lowest S_4 one) is found to be lower in energy than all singlet curves. On the contrary, in the Molybdenum case, the D_2 singlet curve is found to be lower in energy than all triplet curves. From these results, it is clear that no geometrical difference between Molybdenum and Chromium could account for the different behavior of these systems. The essential difference in these unsubstituted species is the relative position of the lowest energy singlet and triplet curves. This may essentially originate from atomic energy for pairing two d electrons: it is near 20,000 cm^{-1} in Cr case, a value substantially higher than that measured in Mo case (16,600 cm^{-1}).

3.5 Conclusion

Theoretical analysis of tetrakis-amido transition metal complexes shows that the experimentally determined structures may be rationalized in terms of coupled rotation of the amido ligands within D_2 or S_4 symmetry point groups. The theoretical geometries agree well with those experimentally determined when available. Finally, the difference between Chromium and Molybdenum complexes probably originates from atomic d-electrons pairing energies.

References

1. Bock H, Borrmann H, Havlas Z, Oberhammer H, Ruppert K, Simon A (1991) Angew Chem Int Ed Engl 30:1678
2. Bruckmann J, Krüger C, Borrmann H, Simon A, Bock H (1995) Zeitschriftfür Kristallographie 210:521
3. Fleurat-Lessard P, Volatron F (1998) J Phys Chem A 102:10151
4. Fleurat-Lessard P, Volatron F (2000) Inorg Chem 39:1849
5. Palacio AA, Alemany P, Alvarez S (1999) Inorg Chem 38:707
6. Bradley DC, Chisholm MH (1976) Acc Chem Res 9:273
7. Hagen K, Holwill CJ, Rice DA, Runnacles JD (1988) Inorg Chem 27:2032
8. Haaland A, Rypdal K, Volden HV, Andersen RA (1992) J Chem Soc Dalton Trans 891
9. Chisholm MH, Cotton FA, Extine MW (1978) Inorg Chem 17:1329
10. Dubberley SR, Tyrell BR, Mountford P (2001) Acta Cryst C57:902
11. Chisholm MH, Cowley AH, Lattman M (1980) J Am Chem Soc 102:46
12. Frisch MJ, Trucks GW, Schlegel HB, Scuseria GE, Robb MA, Cheeseman JR, Zakrzewski VG, Montgomery JA, Stratmann RE, Burant JC, Dapprich S, Millam JM, Daniels AD, Kudin KN, Strain MC, Farkas O, Tomasi J, Barone V, Cossi M, Cammi R, Mennucci B, Pomelli C, Adamo C, Clifford S, Ochtersky J, Petersson GA, Ayala PY, Cui Q, Morokuma K, Malick DK, Rabuck AD, Raghavachari K, Foresman JB, Cioslowski J, Ortiz JV, Stefanov BB, Liu G, Liaschenko A, Piskorz P, Komaromi I, Gomperts R, Martin RL, Fox DJ, Keith T, Al-Laham MA, Peng CY, Nanayakkara A, Gonzalez C, Challacombe M, Gill PMW, Johnson BG, Chen W, Wong MW, Andres JL, Head-Gordon M, Replogle ES, Pople JA (1998) Gaussian 98, Revision A. 1, Gaussian, Inc., Pittsburgh PA
13. Frisch MJ, Trucks GW, Schlegel HB, Scuseria GE, Robb MA, Cheeseman JR, Montgomery JA Jr, Vreven T, Kudin KN, Burant JC, Millam JM, Iyengar SS, Tomasi J, Barone V, Mennucci B, Cossi M, Scalmani G, Rega N, Petersson GA, Nakatsuji H, Hada M, Ehara M, Toyota K, Fukuda R, Hasegawa J, Ishida M, Nakajima T, Honda Y, Kitao O, Nakai H, Klene M, Li X, Knox JE, Hratchian HP, Cross JB, Adamo C, Jaramillo J, Gomperts R, Stratmann RE, Yazyev O, Austin AJ, Cammi R, Pomelli C, Ochterski JW, Ayala PY, Morokuma K, Voth GA, Salvador P, Dannenberg JJ, Zakrzewski VG, Dapprich S, Daniels AD, Strain MC, Farkas O, Malick DK, Rabuck AD, Raghavachari K, Foresman JB, Ortiz JV, Cui Q, Baboul AG, Clifford S, Cioslowski J, Stefanov BB, Liu G, Liashenko A, Piskorz P, Komaromi I, Martin RL, Fox DJ, Keith T, Al-Laham MA, Peng CY, Nanayakkara A, Challacombe M, Gill PMW, Johnson B, Chen W, Wong MW, Gonzalez C, Pople JA (2003) Gaussian 03, Revision B.04 Gaussian, Inc., Pittsburgh PA
14. Ehlers AW, Böhme M, Dapprich S, Gobbi A, Höllwarth A, Jonas V, Köhler KF, Stegmann R, Veldkamp A, Frenking, G (1993) Chem Phys Lett 208:111
15. Titanium orbitals parameters are taken from: Lauher JW, Hoffmann, R (1976) J Am Chem Soc 98:1729
16. Baboul AG, Schlegel, HB (1998) J Phys Chem B 102:5152
17. We were not able to locate the ^2A structures at large angles ($\alpha > 50°$) as well as ^2B structures at small angles ($\alpha < 20°$).
18. For sake of simplicity, we use the terms of D_2 symmetry. The $^3B_2$configuration in D_{2d} group becomes the $^3B_1$ configuration in D_2 group
19. In the Min D_2 structure for singlet Molybdenum, the optimal α value is exactly equal to 30° and this geometry is strictly equivalent to a $D_{2d}90$ structure. For the sake of comparison with the experimental data, the geometrical parameters of this D_2 minimum are given as a $D_{2d}90$ complex